

Tunable Laser Spectra of the Infrared-Active Fundamentals of Cubane

A. S. Pine,^{*†} A. G. Maki,[†] A. G. Robiette,[‡] B. J. Krohn,[‡] J. K. G. Watson,^{||} and Th. Urbanek[§]

Contribution from the Molecular Spectroscopy Division, National Bureau of Standards, Washington, DC 20234, the Department of Chemistry, University of Reading, Whiteknights, Reading, UK RG6 2AD, the University of California, Theoretical Division, Los Alamos National Laboratory, Los Alamos, New Mexico 87545, the Herzberg Institute of Astrophysics, National Research Council of Canada, Ottawa, Ontario, Canada K1A 0R6, and the Institut für Organische Chemie I, Universität Düsseldorf, Düsseldorf, FDR. Received September 19, 1983

Abstract: Confirmation of the octahedral symmetry and improved bond length measurements are obtained from high-resolution tunable laser spectra of the three infrared-active fundamental vibrations of cubane in the vapor phase. The C-H stretching band (ν_{10}) was recorded with a difference-frequency laser and is found to be severely perturbed by a second-order Coriolis resonance with another nearby (nominally inactive) C-H stretch. The C-H bend (ν_{11}) and the C-C stretch (ν_{12}), which were studied with diode lasers, are relatively unperturbed, revealing the symmetry from the nuclear spin weight intensities of the ro-vibrational clusters and the bond lengths from an analysis of the rotational fine structure. The data also provided the f_{1u} -block ζ constants, which have been used, together with vibrational fundamentals from an earlier solid-state study of cubane and its isotopic derivatives, to determine a quadratic force field for the molecule which results in some minor reassessments of the modes.

To structural chemists, cubane is one of the most intriguing of all organic molecules because of its high symmetry and unique bonding. As its name implies, cubane has a skeleton of eight carbon atoms located at the vertices of a cube, each bonded to three others at 90° (instead of the usual 109.5° tetrahedral bond angle of a saturated hydrocarbon) and to a single outboard hydrogen located along the body diagonal. Cubane was first synthesized by Eaton and Cole¹ in 1964; the sample used here was prepared² by using the method given by Chapman et al.³ for a brominated precursor. At room temperature the molecule occurs in the solid phase as millimeter-sized crystallites with rhombohedral facets; the vapor pressure is about 0.5 torr. An X-ray study of the crystal by Fleischer⁴ yielded an average C-C bond distance of 1.551 (5) Å and a C-H bond length of 1.06 (7) Å.

In the isolated molecule there are 18 fundamental vibrational modes, listed in Table I, but the cubic symmetry (O_h) restricts the infrared activity to but 3 of these and the Raman activity to 8. In the solid phase, the rhombohedral distortion of the molecule by its crystal neighbors activates the remaining modes and splits some degeneracies. This has enabled Della et al.⁵ in a thorough infrared and Raman study of the vibrational spectra of solid cubane and four deuterium-substituted derivatives, to determine all of the vibrational mode wavenumbers listed in the first column of Table I along with their symmetries and dominant characters. More recently, Cole et al.⁶ examined the three infrared-active f_{1u} modes in the vapor phase at moderate resolution ($\sim 0.06 \text{ cm}^{-1}$ unapodised) with a Fourier transform interferometer in order to obtain rotation-vibration constants. Though unable to resolve the octahedral fine structure expected for a spherical top molecule, they were able to distinguish the J manifolds, resulting in reasonable rotational constants and band centers. We have recorded all three infrared-active fundamentals at Doppler-limited resolution using tunable laser instrumentation. The two lower frequency modes—namely the C-C stretch, ν_{12} , at 852 cm^{-1} and the C-H bend, ν_{11} , at 1235 cm^{-1} —were studied with Pb-salt diode lasers, whereas the high-frequency C-H stretch, ν_{10} , at 2990 cm^{-1} was recorded with a difference-frequency spectrometer.⁷ Octahedral fine structure is observed in all three bands, but assignments and complete analyses have been accomplished as yet only for the lower

Table I. Vibrational Fundamentals (cm^{-1}) of Cubane (C_8H_8)

solid ^a	vapor ^b	mode	symmetry	activity ^c	approximate description
2995		ν_1	a_{1g}	R, p	C-H
2978	2990	ν_{10}	f_{1u}	IR	C-H
~2978		ν_3	a_{2u}	C-H	
2970		ν_{13}	f_{2g}	R, dp	C-H
1230	1235	ν_{11}	f_{1u}	IR	
1182		ν_{14}	f_{2g}	R, dp	
1151		ν_7	e_u		
1130		ν_9	f_{1g}		
1083		ν_5	e_g	R, dp	
1036		ν_{17}	f_{2u}		
1002		ν_2	a_{1g}	R, p	C-C
912		ν_6	e_g	R, dp	C-C
853	852	ν_{12}	f_{1u}	IR	C-C
839		ν_4	a_{2u}		
829		ν_{18}	f_{2u}		
821		ν_{15}	f_{2g}	R, dp	
665		ν_{16}	f_{2g}	R, dp	
617		ν_8	e_u		

^a Reference 5. ^b Reference 6. ^c IR = infrared, R = Raman, p = polarized, dp = depolarized.

two bands which are relatively unperturbed. Hence we concentrate on the diode laser results in this paper since much structural

[†]National Bureau of Standards

[‡]University of Reading.

^{||}Los Alamos National Laboratory.

[§]National Research Council of Canada.

[¶]Institut für Organische Chemie I.

(1) P. E. Eaton and T. W. Cole, Jr., *J. Am. Chem. Soc.*, **86**, 3157-3158 (1964).

(2) H.-D. Martin, P. Pföhler, T. Urbanek, and R. Walsh, *Chem. Ber.*, **116**, 1415-1421 (1983).

Table II. Nuclear Spin Statistical Weights in Cubane (C_8H_8)

species	weight ^{a,b}
Single Levels	
A ₁	23
A ₂	13
E	20
F ₁	27
F ₂	33
Clusters	
A ₁ + F ₁ + F ₂ + A ₂	96
F ₁ + E + F ₂	80
F ₂ + E + F ₁	80
A ₁ + F ₁ + E	70
F ₁ + F ₂	60
E + F ₂ + A ₂	66
F ₂ + F ₁	60

^a Reference 9. ^b Reference 10.

information has been obtained from them.

Because of the simplifying effects of its high symmetry, cubane may well be the largest molecule (in terms of numbers of atoms) for which the rotational structure will ever be resolvable at the Doppler limit. Benzene⁸ was the former record holder, whereas most chain hydrocarbons with four or more carbons yield only a dense, unresolvable continuum with Doppler-limited or lower resolution. Also fortuitously, the very rigid carbon framework of cubane causes the lowest frequency carbon deformation modes to occur above 600 cm⁻¹. This results in only a modest thermal population of about 6 and 7% for the lowest ν_8 and ν_{16} modes, respectively, at room temperature and a ground-state occupancy of nearly 61%. Thus hot bands do not interfere significantly with the spectra of the fundamentals, although they are in evidence. Another minor complication arises from the ¹³C isotope in 1.1% natural abundance which leads to an 8.9% population for ¹³C₁₂¹²C₇H₈ relative to pure ¹²C₈H₈.

The prior X-ray data⁴ and low-resolution spectra^{5,6} were certainly indicative of and consistent with the cubic symmetry of the molecule, but were not conclusive. The high-resolution spectrum can, however, establish with certainty the cubic symmetry from the spin-statistical weights of the octahedral fine structure transitions due to the eight indistinguishable hydrogens and carbons. The spin weights have been worked out recently by Balasubramanian et al.⁹ and independently by Weber¹⁰ with the results shown in Table II. As is characteristic of heavy spherical top spectra, many individual ro-vibrational transition fall into nearly degenerate clusters corresponding to molecular rotations about high-symmetry threefold or fourfold axes.¹¹ These clusters exhibit distinctive intensity alternation patterns, also given in Table II, which help to establish the *J* assignments. The cluster intensity patterns for cubane show less dramatic alternation than those for smaller spherical tops, such as CH_4 ¹² or SF_6 ,¹³ because of the larger number of possible spin wave function combinations. However, they are readily discernible in the diode laser spectra as illustrated in Figure 1 by the R(36) manifold of ν_{12} , which conclusively

(3) N. B. Chapman, J. M. Key, and K. J. Toyne, *J. Org. Chem.*, **35**, 3860-3867 (1970).
 (4) E. B. Fleischer, *J. Am. Chem. Soc.*, **86**, 3889-3890 (1964).
 (5) E. W. Della, E. F. McCoy, H. K. Patney, G. S. Jones, and F. A. Miller, *J. Am. Chem. Soc.*, **101**, 7441-47457 (1979).
 (6) T. W. Cole, Jr., J. Perkins, S. Putnam, P. W. Pakes, and H. S. Strauss, *J. Phys. Chem.*, **85**, 2185-2189 (1981).
 (7) A. S. Pine and A. G. Robiette, to be published.
 (8) J. Pliva and A. S. Pine, *J. Mol. Spectrosc.*, **93**, 209-236 (1982).
 (9) K. Balasubramanian, K. S. Pitzer, and H. S. Strauss, *J. Mol. Spectrosc.*, **93**, 447-449 (1982).
 (10) A. Weber, private communication.
 (11) W. G. Harter and C. W. Patterson, *J. Chem. Phys.*, **66**, 4872-4885, 4886-4892 (1977).
 (12) G. Herzberg, "Infrared and Raman Spectra of Polyatomic Molecules", D. Van Nostrand Co., Princeton, N. J., 1945, Chapter I, Section 3.
 (13) C. D. Cantrell and H. W. Galbraith, *J. Mol. Spectrosc.*, **58**, 158-164 (1975).

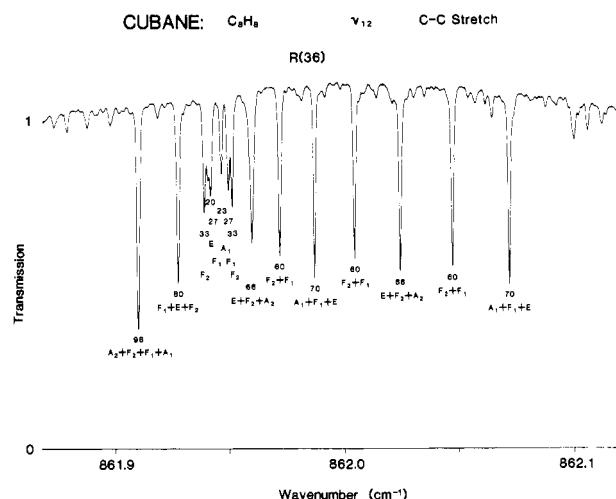


Figure 1. Diode laser transmission trace of the R(36) manifold of the C-C stretching band, ν_{12} , of cubane illustrating alternating intensities due to nuclear spin statistical weights for indicated transitions and clusters.

confirms the cubic symmetry of cubane. This intensity alternation also leads to an unambiguous J assignment for the P- and R-branch manifolds.

Experimental Details

The cubane sample of a few milligrams was stored in an evacuated, sealed-off glass vial and transferred by sublimation under vacuum at liquid nitrogen temperature to another vial with a Kovar-seal mounted stainless steel valve. Other than pumping for a few minutes on the sample held at 77 K, no further purification was attempted or required. The absorption cell was a glass tube 50 cm long by 2.7 cm in diameter with NaCl windows glued on (with Glyptal) at a tilt angle of $\sim 10^\circ$ to avoid spectral channeling. The cell stopcock had a greaseless Teflon seat, since Della et al.⁵ cautioned against cubane dissolving in stopcock grease. The absorption cell was filled with 0.50 torr of cubane at room temperature, and no sample degradation was observed over a period of more than 1 month. Spectral measurements were performed at $T = 296$ K in a single-pass geometry; absorption depths ranged from 10 to 60% for the measured allowed lines.

Spectra of the C-H stretching band were recorded with a scan-controlled difference-frequency laser⁷ with digital data acquisition and processing. Complete coverage, base line normalization, Beer's law correction, and precision calibration against CH₄¹⁴ standards were achieved for this band. For the lower frequency bands, Pb-salt diode lasers were obtained commercially¹⁵ and were used with a monochromator mode sorter and HgCdTe detectors. Two diodes were employed, one for each band, yielding 30–40% coverage, which was an adequate random sample in both cases to obtain a useful analysis. Calibration was accomplished by reference to OCS¹⁶ absorption lines in the 850-cm⁻¹ region and N₂O¹⁷ lines near 1235 cm⁻¹ with use of an ~7.5 cm long temperature-controlled germanium etalon for interpolation. All scans were within 0.5 cm⁻¹ of a reference line, the scans being limited primarily by diode laser mode-hopping and thermal stability. Slow thermal drifts of the etalon were partially compensated by averaging two sequential scans in opposite directions. These drifts, plus subsidiary mode leakage and diode laser amplitude fluctuations (chiefly from mode competition), limited the wavenumber precision to ~±0.0003 cm⁻¹ as determined from out least-squares fitting. Uncertainties in the absolute calibration contribute an additional uncertainty in the band center of ±0.0001 cm⁻¹ for ν_{12} and ±0.0003 cm⁻¹ for ν_{11} . Line centers were read from charts with an HP9825 computer/digitizer. No base line corrections were applied to the diode laser data shown here.

Spectra

Spectra Figures 2 and 3 show several illustrative traces of R- and P-branch manifolds for the ν_{11} and ν_{12} bands of cubane. In Figure 2a we note the reversal of the R(36) pattern for ν_{11} compared to that of ν_{12} in Figure 1. This indicates that the sign of g , the

(14) G. Tarrago, M. Dang-Nhu, G. Poussique, G. Guelachvili, and C. Amiot, *Mol. Phys.*, **57**, 246-263 (1975).
 (15) Laser Analytics Division of Spectra-Physics, Bedford, MA.
 (16) A. G. Maki, J. S. Wells, F. R. Peterson, W. B. Olson, A. Fayt, and J. P. Sattler, *J. Phys. Chem. Ref. Data*, in press.
 (17) G. Guelachvili, *Can. J. Phys.*, **60**, 1334-1347 (1982).

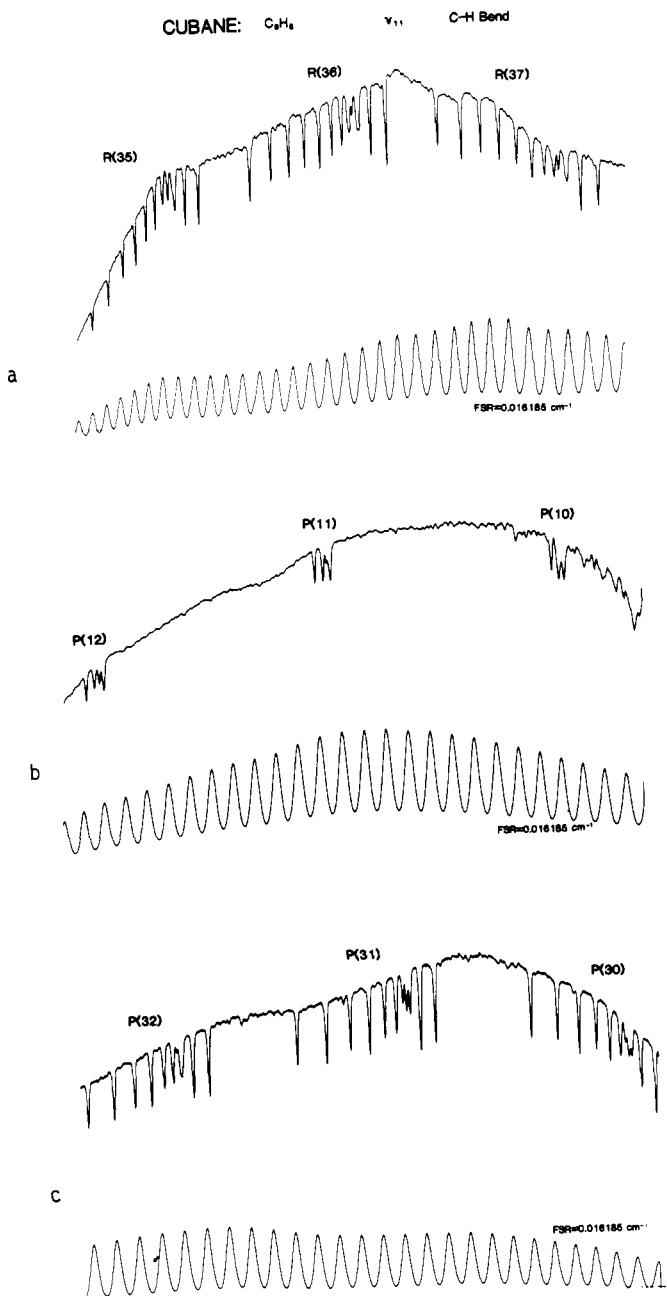


Figure 2. Diode laser transmission traces for selected J manifolds in the P and R branches of the C-H bending band, ν_{11} , of cubane. Frequency increases to the right.

octahedral splitting coefficient, is opposite for the two bands and roughly equal in magnitude. The lower J P-branch manifolds in Figure 2b exhibit an extraneous feature to the high-frequency side of P(10), seen also in the lower resolution ν_{11} spectrum of Cole et al.,⁶ which probably arises from either a hot band or a $^{13}\text{C}^{12}\text{C}_2\text{H}_8$ isotope band. As will be shown below, the ν_{11} Q branch itself is quite narrow for transitions from the ground vibrational state, comprising only the single strongest peak in the Cole⁶ spectrum, and cannot account for the structure near P(10). The alternating cluster intensity ratios are again evident for the higher J P-branch manifolds of ν_{11} shown in Figure 2c.

The ν_{12} -band manifolds shown in Figure 3 are similar but exhibit some marked deviations from the regular spherical top F_4 patterns usually encountered.¹⁸ First we note that the high J manifolds near R(43) in Figure 3a are nearly overlapping whereas the P manifolds in Figure 3c up to $J \sim 52$ are still well separated.

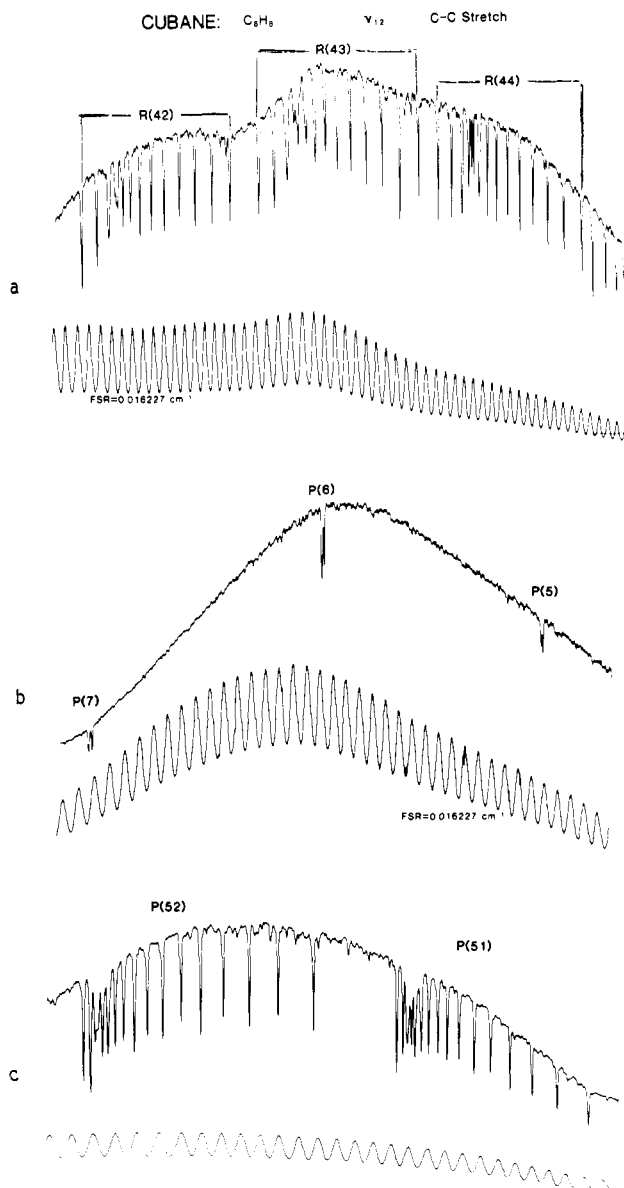


Figure 3. Diode laser transmission traces for selected J manifolds in the P and R branches of the C-C stretching band, ν_{12} , of cubane. Frequency increases to the right.

Without centrifugal distortion and other perturbations, the P-branch manifolds would overlap at lower J than the R-branch manifolds. Also the F_4 patterns of the P(51) and P(52) manifolds themselves are severely compressed on the threefold (left or lower wavenumber) side, indicative, of a perturbation requiring higher-order terms in the theoretical fit. The low J P-branch multiplets in Figure 3b illustrate that the Q-branch tail is not extensive and that the spectra are relatively free of interfering isotope and hot bands. Because of diode laser idiosyncrasies, we were not able to scan the Q branch of ν_{12} . As will be seen later, however, we do obtain some Q-branch information because of the mixing between the Coriolis sublevels in this band.

In Figure 4 we show the observed Q branch of ν_{11} , the C-H bend, compared to a simulated spectrum based on the very simple model^{18,19}

$$\nu_Q = m + vJ(J + 1) - 2gQ_4 \quad (1)$$

where the band center, m , and the octahedral splitting constant, g , are determined from the P and R branches discussed later. Q_4 is a symmetry-adapted vector-coupling coefficient for the Q

(18) B. Bobin and K. Fox, *J. Phys., Lett. (Orsay, Fr.)*, **34**, 571-582 (1973); J. Moret-Bailly, *J. Mol. Spectrosc.*, **15**, 344-354 (1965).

(19) E. G. Brock, B. J. Krohn, R. S. McDowell, C. W. Patterson, and D. F. Smith, *J. Mol. Spectrosc.*, **76**, 301-321 (1979).

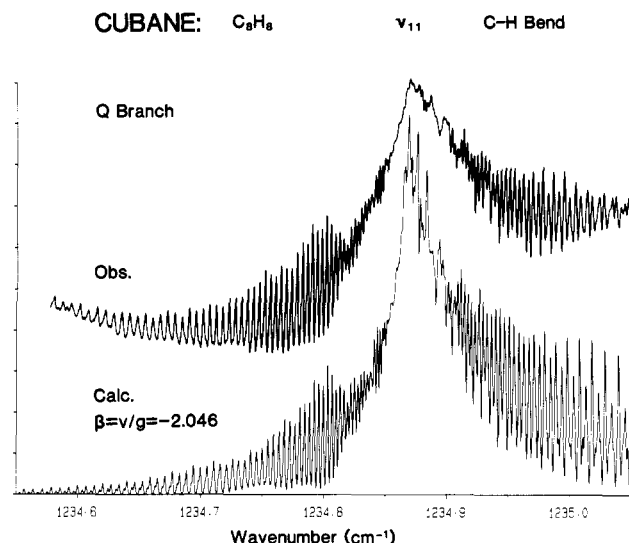


Figure 4. Comparison of the diode laser transmission trace (inverted) for the Q branch of the C-H bending mode, ν_{11} , of cubane with the calculated intensity spectrum for $\beta = 2.046$.

branch¹⁸ and ν , a $B' - B''$ type term, is adjusted for best agreement with experiment. The overall shape of the Q branch depends on the ratio¹⁹ $\beta = \nu/g = -2.046$ (8) and is seen to mimic the data faithfully out to very high J in the wings where centrifugal distortion effects, omitted from the model, become significant. The strong intensity peaks in the center of the Q branch in Figure 4 are somewhat saturated in the observed spectrum since base line and Beer's law corrections were not made. The calculated spectrum is presented with the y axis in absorbance units while the observed spectrum has a percent absorption scale with an absorption of more than 90% at the band center. Fortunately, the observed Q branch appears relatively uncluttered by extraneous isotope and hot-band structure over the range shown. The wavenumber scale in the observed trace is not exactly coincident with the simulation owing to slight nonlinearities in the tuning rate of the diode laser. However, the detailed band contour is very sensitive to the constants because of the extensive blending of clusters, which accounts for the relatively small uncertainty in β above.

Portions of the ν_{10} , C-H stretching, band are presented in Figure 5, illustrating the lack of recognizable F_4 patterns in the P and R branches and the subsidiary Q^+ and Q^- subbranches on either side of the stronger "allowed" Q^0 subbranch.

Analysis

Although the spectra of ν_{11} and ν_{12} exhibit easily recognizable spherical top cluster patterns, neither band is adequately fit by the usual dominant approximation (the diagonal F_4 expansion¹⁸). We use then a third-order perturbation theory approach developed by Krohn and Watson²⁰ summarized by

$$\begin{aligned} \nu_{R,P} = & m + nM + pM^2 + qM^3 + \dots \\ & + (g + hM + kM^2 + \dots)F_4(R,P) \\ & + (z' + z''M + \dots)F_6(R,P) \\ & + f(B\zeta, g, h, (v - p), M, F_4, F_6) \end{aligned} \quad (2)$$

where $M = J + 1$ for the R branch and $M = -J$ for the P branch and J is the ground state angular momentum quantum number. The scalar terms on the first line and the diagonal F_4 and F_6 octahedral coefficients on the second and third lines are augmented by corrections due to off-diagonal matrix elements on the fourth line given in detail in Table II of Krohn and Watson.²⁰ These corrections involve the second-order expansion parameter $g^2/B\zeta$ and the third-order parameters $g^3/(B\zeta)^2$, $g^2(v - p)/(B\zeta)^2$, and $gh/B\zeta$. Thus a nonlinear least-squares fit of this model to the data yields the constants $B\zeta$ and v , which are not ordinarily ob-

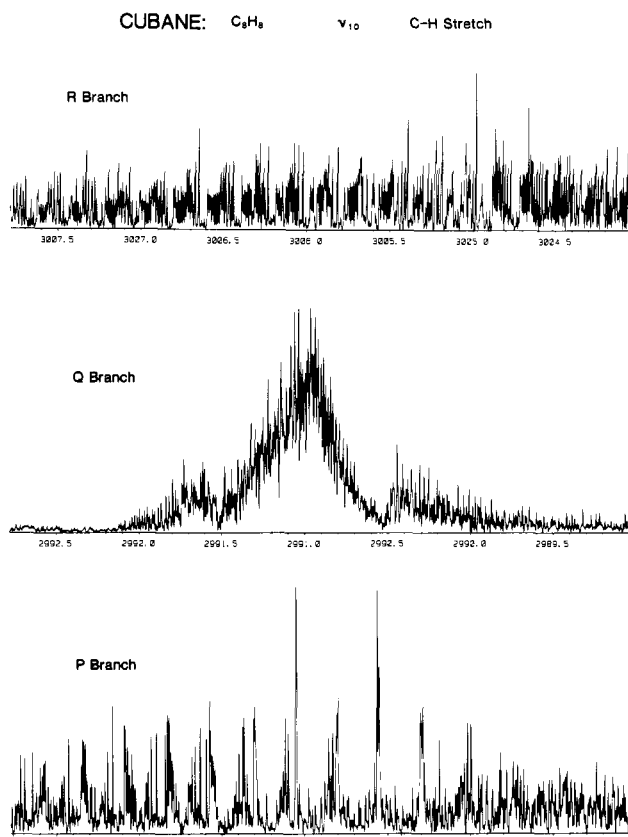


Figure 5. Excerpts of the R, Q, and P branches of the C-H stretching mode, ν_{10} , recorded with a difference-frequency laser spectrometer. The intensity of the Q branch has been reduced by two compared to the P and R branches for convenience in plotting.

tained from the P and R branches of an unperturbed infrared band of a spherical top. The convergence of the fit depends on the smallness of the perturbation theory expansion parameters. For the ν_{11} and ν_{12} bands of cubane the convergence is rapid (two iterations) and the results are presented in Table III. Parenthetically we note here that for the C-H stretching band, ν_{10} , where $\zeta \sim 0$, the above expansion is inappropriate and a full diagonalization will be required. Omitted from the ν_{11} and ν_{12} fits were certain sums over off-diagonal F_4 coefficients²⁰ which have not yet been tabulated. These contributions, which can be described as the second-order effects of an off-diagonal second-order contribution within a near-degenerate set, have a fourth-order numerator and a first-order denominator.²⁰ These corrections for cubane have been estimated as $< 5 \times 10^{-6} \text{ cm}^{-1}$ for $J < 55$, and so are entirely negligible compared to the measurement precision.

The overall root mean square error for the fit to 722 transitions (300 measured lines or clusters) of the ν_{12} band is $3.3 \times 10^{-4} \text{ cm}^{-1}$ and that to 580 transitions (248 measured lines or clusters) of the ν_{11} band is $2.6 \times 10^{-4} \text{ cm}^{-1}$. The least-squares weighting for unresolved clusters was proportional to the relative spin weights of the transition components. A few threefold clusters in the high $J (> 50)$ P-branch manifolds of ν_{12} were given reduced or zero weights because of observed - calculated wavenumber residuals greater than three times the root mean square error, which indicates the presence of a local resonant perturbation. The slightly worse fit of the ν_{12} band probably reflects this perturbation.

The most likely candidate for the perturbation of ν_{12} is a first-order Coriolis resonance with ν_{18} (f_{2u} , 829 cm^{-1}) lying just 24 cm^{-1} below. The force-field calculation described later yields a rather large Coriolis coupling constant, $|\zeta_{12,18}| = 0.435$, between these two vibrations. A higher-order rotational perturbation of ν_{12} by the even closer ν_4 (a_{2u} , 839 cm^{-1}) is also possibility. On the other hand, ν_{11} is relatively isolated, being about 90 cm^{-1} above the nearest u species fundamental, ν_7 (e_u , 1151 cm^{-1}), which could participate in a Coriolis interaction. Possible candidates for a

(20) B. J. Krohn and J. K. G. Watson, to be published.

Table III. Vibration-Rotation Constants (cm⁻¹) for Cubane

	C-C stretch		C-H bend	
	ν_{12}^a	ν_{12}^b	ν_{11}^a	ν_{11}^b
<i>m</i>	851.82750 (5) ^c	851.279 (8)	1234.86714 (3)	1234.670 (2)
<i>n</i>	0.2698460 (17)	0.26968 (4)	0.1734839 (17)	0.17338 (4)
<i>p/10⁻⁴</i>	1.30935 (46)	1.160 (5)	0.51243 (35)	0.750 (8)
<i>q/10⁻⁷</i>	-3.848 (13)	-2.68 (4)	-0.481 (20)	-0.083 (4)
<i>g/10⁻⁵</i>	2.3955 (38)		-2.2504 (14)	
<i>h/10⁻⁷</i>	1.5220 (27)		0.318 (38)	
<i>k/10⁻¹⁰</i>	-7.48 (17)			
<i>z'/10⁻¹⁰</i>	1.199 (19)		0.096 (38)	
<i>z''/10⁻¹³</i>	-4.77 (49)			
<i>v/10⁻⁴</i>	1.564 (92)		0.461 (2) ^d	
<i>Bξ/10⁻²</i>	-2.247 (31)	-1.786 (?) ^e	2.511 (49)	2.993 (?) ^e

^a Present work. ^b Reference 6. ^c Errors in parentheses are one standard deviation. ^d From Q-branch simulation. ^e Estimated in ref 6 by using the ξ sum rule; no errors stated.

Fermi-type resonance are for the most part well above ν_{11} , the nearest being $\nu_8 + \nu_{16}$ (~ 1282 cm⁻¹).

Also in Table III we compare our present results with the lower resolution Fourier transform spectrum results of Cole et al.⁶ Since they did not resolve the octahedral splittings, they could obtain only the scalar constants. The rotational constants are in reasonable agreement, but their band centers are too low—probably reflecting a missassignment of the *J* values by 2 for ν_{12} and 1 for ν_{11} , rather than a miscalibration. In the present study all the parameters listed are statistically well determined except for *z'* in ν_{11} which is marginally about three standard deviations. Also the parameter *v* could not be determined with statistical significance in the ν_{11} fit, so it was fixed to the value obtained from the Q-branch simulation. Note that for ν_{12} , *v* is well determined (and relatively uncorrelated with its partner, *p*) even though we have not measured the Q branch.

The relationships between the fitting parameters *n*, *p*, *v*, etc., and the more usual molecular constants are to a good approximation

$$n = B_v + B_0 - 2B\xi_v \quad (3)$$

$$(2p + v)/3 = B_v - B_0 \quad (4)$$

The values of *n*, *p*, *v*, and $B\xi_v$ given in Table III can be used to derive the ground-state *B* value. We obtain $B_0 = 0.11183$ (25) cm⁻¹ from ν_{11} , and $B_0 = 0.11238$ (16) cm⁻¹ from ν_{12} . The error limits on B_0 arise from the experimental uncertainties in $B\xi_v$. A weighted mean value of B_0 from the two bands is $B_0 = 0.1122$ (2) cm⁻¹, which in turn leads to $\xi_{11} = 0.224$ (4) and $\xi_{12} = -0.200$ (3).

The ξ sum rule, $\xi_{10} + \xi_{11} + \xi_{12} = 0$, for the three f_{1u} modes^{6,21} yields $\xi_{10} \sim -0.024$ for the C-H stretching mode, ν_{10} . This small value of ξ_{10} , along with the very close proximity of the a_{2u} symmetry C-H stretching mode, ν_3 , leads to the extremely perturbed spectrum of ν_{10} seen in Figure 5. The coupling between the f_{1u} and a_{2u} modes is through a second-order Coriolis operator of the kind

$$q_3[q_{10x}(J_yJ_z + J_zJ_y)] + \text{cyclic permutations}$$

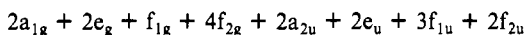
analogous to the ν_1/ν_3 coupling observed for the “local” hydrogen stretching modes in silane and germane.²²⁻²⁶ The other C-H stretching modes of *g* parity cannot perturb ν_{10} in any way. Furthermore, since all remaining fundamentals are less than 1250 cm⁻¹, strong resonances with binary combinations cannot occur.

Force-Field Calculations

The ξ constants provide valuable information on the quadratic

- (21) R. S. McDowell, *J. Chem. Phys.*, **43**, 319-323 (1965).
- (22) A. Cabana, D. L. Gray, I. M. Mills, and A. G. Robiette, *J. Mol. Spectrosc.*, **66**, 174-176 (1977).
- (23) A. Cabana, D. L. Gray, A. G. Robiette, and G. Pierre, *Mol. Phys.*, **36**, 1503-1516 (1978).
- (24) A. Owyoung, P. Esherick, A. G. Robiette, and R. S. McDowell, *J. Mol. Spectrosc.*, **86**, 209-215 (1981).
- (25) P. Lepage, J. P. Champion, and A. G. Robiette, *J. Mol. Spectrosc.*, **89**, 440-448 (1981).
- (26) S. Q. Mao, R. Saint-Loup, A. Aboumajd, P. Lepage, H. Berger, and A. G. Robiette, *J. Raman Spectrosc.*, **13**, 257-261 (1982).

force field. The 18 normal modes of cubane span the representation^{5,6}



so that only the f_{1u} (infrared-active) and f_{2g} (Raman-active) blocks involve more than a 2×2 G-F calculation. A complete harmonic force field calculation has been carried out, using as data the solid-state vibrational wavenumbers measured by Della et al.⁵ for cubane-*d*₀, cubane-*d*₂, cubane-*d*₆, and cubane-*d*₈, together with the gas-phase ξ_{11} and ξ_{12} for cubane-*d*₀ determined here.

Full details of the force-failed work, i.e., the coordinates used to represent the force field and the interpretation of the potential constants obtained, will be published elsewhere.²⁷ For the purposes of this paper we note only that all force constants are well determined by the data apart from those in the 4×4 f_{2g} block (where at present one constraint has been made): gas-phase ξ constants for the f_{2g} modes are needed to remove the indeterminacy in this block. Illustrative results from the force-field refinement are given in Tables IV and V. Table IV shows the wavenumber fit achieved for the four isotopic species included. The experimental data on the vibrational modes of cubane-*d*₁, and the more tentative and incomplete assignments for cubane-*d*₄, cubane-*d*₅, cubane-*d*₇, and ¹³C-substituted species, are also well reproduced. A few of the assignments of Della et al.⁵ have been revised, notably the f_{2u} modes of cubane-*d*₈ and two cubane-*d*₆ fundamentals which correlate with these. It is also possible that minor changes are still needed in some of the fundamentals lying between 800 and 850 cm⁻¹ in cubane-*d*₀, -*d*₁, and -*d*₂. On the whole, however, the force-field calculation confirms the earlier assignments quite satisfactorily.

Table V gives more details of the f_{1u} and f_{2g} blocks of cubane-*d*₀ and cubane-*d*₈. The sums of the calculated ξ constants are in agreement with those derived by McDowell,²¹ and individual ξ 's fall within the limits given by McDowell in a later paper.²⁸ For the case of cubane these are $-1/2 \leq \xi_v \leq +1$ in both the f_{1u} and f_{2g} blocks. McDowell's results also require that $\xi_v = +1/2$ for the single f_{1g} mode and both f_{2u} modes in any isotopic species of cubane with *O*_h symmetry, irrespective of the force field. This was found to be so at all stages of the calculations.

The force field also yields information about the character of the ν_{11} and ν_{12} modes which we have analyzed. Cole et al.⁶ drew attention to the f_{1u} ξ 's expected for hypothetical “pure” normal coordinates, i.e., 0 for a C-H stretching mode, +0.5 for a C-H bending mode, and -0.5 for a C-C stretching mode. The observed ξ_{11} and ξ_{12} for C₈H₈ (+0.22 and -0.20, respectively) show that there is appreciable mixing between the f_{1u} C-H bending and C-C stretching coordinates, but it is clear that ν_{11} is best described as C-H bending and ν_{12} as C-C stretching as previous authors have done. The mixed nature of the normal modes is also shown by the substantial isotope shift in both ν_{11} and ν_{12} on going from C₈H₈ to C₈D₈. In fact the calculated ξ 's for C₈D₈ (Table V) suggest

(27) A. G. Robiette and I. M. Mills, unpublished work.

(28) R. S. McDowell, *J. Chem. Phys.*, **46**, 1535-1536 (1967).

Table IV. Calculated Vibrational Fundamentals (cm^{-1}) of Cubane- d_0 , - d_2 , - d_6 , and - d_8 , Compared with Solid-State Experimental Data^{a-c}

D_{3d} symmetry species	d_0 calcd	o-c	d_2 calcd	o-c	d_6 calcd	o-c	d_8 calcd	o-c
A_{1g}	3017 (A_{1g})	-22	3011	-18	2996	-18	2240 (A_{1g})	19
	2992 (F_{2g})	-22	2220	17	2232	22	2208 (F_{2g})	24
	1182 (F_{2g})	0	1174	0	1081	2	1072 (F_{2g})	0
	1003 (A_{1g})	-1	991	0	967	0	955 (A_{1g})	1
	826 (F_{2g})	-5	819	2	725	0	711 (F_{2g})	4
	665 (F_{2g})	0	654	-3	581	-2	578 (F_{2g})	8
A_{2g}	1131 (F_{1g})	-1	1131	(0)	883	1	883 (F_{1g})	1
E_g	2992 (F_{2g})	-22	2991	-21	2210	19	2208 (F_{2g})	24
	1182 (F_{2g})	0	1169	-1	1146	-1	1072 (F_{2g})	0
	1131 (F_{1g})	-1	1099	1	1035	0	1027 (E_g)	0
	1085 (E_g)	-2	1014	2	983	2	883 (F_{1g})	1
	913 (E_g)	-1	878	-3	755	3	711 (F_{2g})	4
	826 (F_{2g})	-5	740	-2	702	2	682 (E_g)	2
A_{1u}	665 (F_{2g})	0	632	0	602	-4	578 (F_{2g})	8
	1036 (F_{2u})	0	1036	0	977	-2	977 (F_{2u})	(0)
	829 (F_{2u})	0	829	9	622	1	622 (F_{2u})	1
	829 (F_{2u})	0	829	9	622	1	622 (F_{2u})	1
A_{2u}	2998 (F_{1u})	-20	2995	-27	2997	-23	2221 (A_{2u})	(18)
	2994 (A_{2u})	(-16)	2219	21	2220	22	2217 (F_{1u})	23
	1230 (F_{1u})	0	1220	2	1101	-1	1082 (F_{1u})	1
	855 (F_{1u})	-2	849	2	811	-4	802 (A_{2u})	5
	841 (A_{2u})	-2	824	3	688	2	683 (F_{1u})	3
	1230 (F_{1u})	0	1205	-4	1162	2	1082 (F_{1u})	1
E_u	2998 (F_{1u})	-20	2998	-21	2217	19	2217 (F_{1u})	23
	1150 (E_u)	0	1111	-2	1014	0	977 (F_{2u})	(0)
	1036 (F_{2u})	0	993	2	972	3	958 (E_u)	2
	855 (F_{1u})	-2	845	-1	791	-5	683 (F_{1u})	3
	829 (F_{2u})	0	712	-1	650	1	622 (F_{2u})	1
	618 (E_u)	-1	574	0	537	1	525 (E_u)	2

^a For cubane- d_0 and - d_8 the O_h symmetry species are indicated. The underlining of a calculated wavenumber implies a change in assignment from earlier work. ^b Columns headed o-c are observed - calculated differences, with observed wavenumbers taken from ref 5. A difference in parentheses indicates that the wavenumber was estimated from the product rule rather than observed directly.

Table V. Calculated Wavenumbers and ξ Constants of the f_{1u} and f_{2g} Blocks of Cubane- d_0 and Cubane- d_8

symmetry	r	C_8H_8		C_8D_8	
		ν_r (cm^{-1})	ξ_r ^b	ν_r (cm^{-1})	ξ_r
f_{1u}	10	2998.3	-0.023	2217.2	-0.053
	11	1230.3	0.224	1082.3	-0.032
	12	855.2	-0.201	682.8	0.084
f_{2g}	13	2992.0	-0.088	2207.9	-0.074
	14	1182.2	0.857	1071.9	0.944
	15	826.2	0.412	711.5	-0.335
	16	665.4	-0.181	577.8	0.465

^a The calculated ξ constants for the f_{1g} mode and both f_{2u} modes in C_8H_8 and C_8D_8 are all +0.5, in agreement with the sum rules and limiting values derived by McDowell (cf. ref 20 a and 21). ^b The calculated f_{1u} ξ constants for C_8H_8 should be compared with the observed values, i.e., ξ_{11} (obsd) = +0.224, ξ_{12} (obsd) = -0.200 (see text); the sum rule would imply ξ_{10} (obsd) = -0.024.

that in the fully deuterated molecule the C-D bending and C-C stretching are mixed essentially 50/50, since both ξ_{11} and ξ_{12} are close 0.

Molecular Structure

Since we have confirmed the cubic symmetry of cubane, only the C-C and C-H bond lengths are required to specify the structure of the molecule; these are designated here by R and r respectively for the ground vibrational state. The moment of inertia is then

$$I_0 = 4(M_C + M_H)R^2 + (16M_H/3^{1/2})[rR + (r^2/3^{1/2})] \quad (5)$$

which is related to the ground-state B_0 value by

$$B_0 = \hbar/8\pi^2 c I_0 \quad (6)$$

B_0 has been determined here for only one isotopic species, so we must make an assumption about one of the bond lengths in order to determine the other.

The molecule closest in structure to cubane studied earlier is probably *syn*-tricyclo[4.2.0.0^{2,5}]octane, for which Andersen and Fernholz²⁹ found mean bond lengths of r_a (CH) = 1.111(7) Å and r_a (CC) = 1.566 (3) Å by electron diffraction. If we take for cubane r = 1.11 (2) Å, then from eq 5 and 6 we obtain R = 1.565 (4) Å using our value for B_0 = 0.1122 (2) cm^{-1} , in excellent correspondence with r_a (CC) above. A recent ab initio investigation of cubane by Almlöf and Jonvik,³⁰ believed to be close to the Hartree-Fock limit, gave a C-C bond length of 1.570 Å. The latter authors commented that the bond lengths obtained by X-ray diffraction may be shorter than the true bond lengths, as neither libration nor bonding effects on the electron density distribution were explicitly considered in the X-ray study. Thus even though the X-ray value of 1.551 (5) Å for the C-C bond in the crystal⁴ is considerably lower than our gas-phase value, we are reasonably confident in our value, particularly since it is within the range (1.555–1.566 Å) determined for other four-membered-ring hydrocarbons.³¹

The influence on the C-C bond length by the assumption of the C-H bond length is relatively small since, by virtue of their lighter mass, the hydrogens have less leverage on I_0 . An uncertainty in r leads to a reduced uncertainty in R by the ratio

$$dR/dr = -2y/3^{1/2}[y + (M_C/M_H)] \sim -0.142 \quad (7a)$$

(29) B. Andersen and L. Fernholz, *Acta Chem. Scand.*, **24**, 445–452 (1970).

(30) J. Almlöf and T. Jonvik, *Chem. Phys. Lett.*, **92**, 267–270 (1982).

(31) J. H. Callomon, E. Hirota, K. Kuchitsu, W. J. Lafferty, A. G. Maki, and C. S. Pote, Eds., "Structure Data of Free Polyatomic Molecules", Springer-Verlag, Berlin, 1976, Landolt-Bornstein New Series, Vol. II/7.

with

$$y = 1 + (2r/3^{1/2}R) \quad (7b)$$

as obtained from eq 5 by zeroing the variation in I_0 . The assumption about r could be eliminated altogether in future work on isotopic variants of cubane. C_8D_8 would be an obvious possibility, but a symmetric top species such as C_8H_7D , C_8HD_7 , or $^{13}C^{12}C_7H_8$ might in practice prove easier. The ^{13}C species could be examined in natural abundance if a suitable band could be found.

It should also be mentioned that our present uncertainty in B_0 from the perturbation theory fit to ν_{11} and ν_{12} of C_8H_8 might be reduced by an analysis of the present spectrum of the ν_{10} band. This band is so extensively perturbed that the usual concepts of "allowed" and "forbidden" transitions become meaningless, and so assignment of this band should yield numerous ground-state combination differences leading to a higher precision B_0 value as well as ground-state octahedral splitting and centrifugal distortion parameters.

Registry No. Cubane, 277-10-1.

Rotational Spectroscopy of Molecular Complexes of BF_3 with $NCCN$, CO_2 , and N_2O^\dagger

K. R. Leopold, G. T. Fraser, and W. Klemperer*

Contribution from the Department of Chemistry, Harvard University, Cambridge, Massachusetts 02138. Received July 27, 1983

Abstract: The microwave spectrum of the van der Waals complex $NCCN \cdot BF_3$ has been obtained by molecular beam electric resonance spectroscopy. This molecule is shown to be a symmetric rotor. The rotational constants for the ^{11}B and ^{10}B species are $B_0 = 672.2$ (2) and 675.6 (2) MHz, respectively. These values are consistent with a B-N bond length of 2.647 (3) Å. Radio-frequency and microwave transitions of the complex $CO_2 \cdot BF_3$ have been observed and establish that this molecule is an asymmetric rotor. One radio-frequency transition observed for $N_2O \cdot BF_3$ suggests an asymmetric structure for this complex as well.

Introduction

Addition complexes of the strong Lewis acid- BF_3 are fundamental in classical donor-acceptor chemistry. Recently the van der Waals complexes of BF_3 with Ar, CO, and N_2 have been formed in an adiabatic expansion and structurally characterized by their microwave spectra.¹ The van der Waals bonds form along the C_3 axis of the BF_3 in a manner analogous to the binding in the "classical complexes". This behavior seems chemically reasonable and suggests that the van der Waals interaction may also be viewed in terms of a Lewis acid-base model. Such a picture has successfully provided an intuitive understanding of van der Waals interactions in a variety of weakly bound systems.

In view of the chemical character of weakly bound systems it seems reasonable to consider whether, in fact, there is a smooth transition between van der Waals and covalent bonding. Despite structural similarities between the covalent and van der Waals complexes of BF_3 , for example, dramatic differences exist. The B-N bond length in BF_3 -amines is 1.6 Å while that in $N_2 \cdot BF_3$ is 2.9 Å. Such a large variation in bond length with nitrogen donor may permit, at least in principle, the observation of a smooth transition between "covalent" and "van der Waals" binding, provided the nature of the nitrogen donor were properly chosen. Two classes of nitrogen donors which may be used for this purpose are the amines and the cyanides. Microwave data for a number of the gas-phase amines are available, but the analogous data for the cyanides are lacking. With the simplest of these, HCN and CH_3CN , BF_3 forms solid compounds. Cyanogen, on the other hand, does not form a solid with BF_3 , and so was chosen as an interesting system to study.

The structure of $NCCN \cdot BF_3$ is also of interest for comparison with a number of other previously studied "van der Waals" molecules. Recent rotational spectroscopic studies of $CO_2 \cdot HF^2$ and $NCCN \cdot HF^3$, as well as $SCO \cdot HF^2$ and $CO_2 \cdot HCl^4$, have shown these complexes to have linear, hydrogen bonded structures. The linear structures of the $CO_2 \cdot HX$ complexes are not readily un-

derstandable from consideration of oxygen lone pairs on CO_2 , as might be expected if chemical reasoning were applicable. Moreover, the geometry of the closely related, isoelectronic species N_2OHF is quite different, having a bent, hydrogen bonded structure. In view of the similarities between CO_2 and N_2O and the dissimilarities in their complexes with HF, a simple HOMO-LUMO approach does not appear applicable to these systems, since any argument based on lone pairs would have to predict the same structure for N_2OHF and CO_2HF . In contrast, HF and BF_3 appear quite similar in their weak interactions. For example, studies of the complexes of CO and N_2 with HF and BF_3 show that HF and BF_3 behave similarly as simple Lewis acids. Specifically, viewed as electron-pair acceptors, both HF and BF_3 accept electrons along their symmetry axes. Thus, given the observed behavior of CO_2 with HF, the complex $CO_2 \cdot BF_3$ is expected to be a symmetric top in which the CO_2 axis is coincident with the symmetry axis of the BF_3 . Likewise, the linear structure of $NCCN \cdot HF$ suggests a similar geometry for $NCCN \cdot BF_3$.

We have studied the complexes $NCCN \cdot BF_3$, $CO_2 \cdot BF_3$, and $N_2O \cdot BF_3$ by rotational spectroscopy using the molecular beam electric resonance technique. The spectra show that the complex $NCCN \cdot BF_3$ does indeed have the anticipated C_{3v} structure, while $CO_2 \cdot BF_3$ and $N_2O \cdot BF_3$ do not. This result further emphasizes the complexity of the binding in CO_2 and N_2O systems.

Experimental

A beam of $NCCN \cdot BF_3$ was formed by expanding a mixture of 1% BF_3 and 25% $NCCN$ in Ar through a 25-μm nozzle at room temperature. The stagnation pressure was typically 2.5 atm. Under these conditions,

(1) K. C. Janda, L. S. Bernstein, J. M. Steed, S. E. Novick, and W. Klemperer, *J. Am. Chem. Soc.*, **100**, 8074 (1978).

(2) F. A. Baiocchi, T. A. Dixon, C. H. Joyner, and W. Klemperer, *J. Chem. Phys.*, **74**, 6544 (1981).

(3) A. C. Legon, P. D. Soper, and W. H. Flygare, *J. Chem. Phys.*, **74**, 4936 (1981).

(4) R. S. Altman, T. A. Dixon, M. D. Marshall, and W. Klemperer, *J. Chem. Phys.*, **77**, 4344 (1982).

*This work was supported by the National Science Foundation.